Condensed Matter and Interphases
(Kondensirovannye sredy i mezhfaznye granitsy)

Original articles

DOI: https://doi.org/10.17308/kcmf.2020.22/3076
Received 29 September 2020
Accepted 15 November 2020
Published online: 25 December 2020

ISSN 1606-867X
eISSN 2687-0711

Synthesis and Physicochemical Properties of $Mn_xFe_{3-x}O_4$ Solid Solutions

© 2020 A. S. Korsakova[a], D. A. Kotsikau[b], Yu. S. Haiduk[b]✉, V. V. Pankov[b]

[a]*Research Institute for Physical Chemical Problems of the Belarusian State University, 14 Leningradskaya str., Minsk 220006, Belarus*

[b]*Belarusian State University, 4 Nezavisimosty prosp., Minsk 220030, Belarus*

Abstract

Ferrimagnetic nanoparticles are used in biotechnology (as drug carriers, biosensors, elements of diagnostic sets, contrast agents for magnetic resonance imaging), catalysis, electronics, and for the production of magnetic fluids and magnetorheological suspensions, etc. The use of magnetic nanoparticles requires enhanced magnetic characteristics, in particular, high saturation magnetisation.

The aim of our study was to obtain single-phased magnetic nanoparticles of $Mn_xFe_{3-x}O_4$ solid solutions at room temperature. We also studied the dependence of the changes in their structure, morphology, and magnetic properties on the degree of substitution in order to determine the range of the compounds with the highest magnetisation value.

A number of powders of Mn-substituted magnetite $Mn_xFe_{3-x}O_4$ (x = 0 – 1.8) were synthesized by means of co-precipitation from aqueous solutions of salts. The structural and micro-structural features and magnetic properties of the powders were studied using magnetic analysis, X-ray diffraction, transmission electron microscopy, and IR spectroscopy.

The X-ray phase analysis and IR spectroscopy confirm the formation of single-phase compounds with cubic spinel structures. The maximum increase in saturation magnetization as compared to non-substituted magnetite was observed for $Mn_{0.3}Fe_{2.7}O_4$ (M_s = 68 A·m^2·kg^{-1} at 300 K and M_s = 85 A·m^2·kg^{-1} at 5 K). This is associated with the changes in the cation distribution between the tetrahedral and octahedral cites.

A method to control the magnetic properties of magnetite by the partial replacement of iron ions in the magnetite structure with manganese has been proposed in the paper. The study demonstrated that it is possible to change the magnetisation and coercivity of powders by changing the degree of substitution. The maximum magnetisation corresponds to the powder $Mn_{0.3}Fe_{2.7}O_4$. The nanoparticles obtained by the proposed method have a comparatively high specific magnetisation and a uniform size distribution. Therefore the developed materials can be used for the production of magnetorheological fluids and creation of magnetically controlled capsules for targeted drug delivery and disease diagnostics in biology and medicine (magnetic resonance imaging).

Keywords: solid solution, magnetic nanoparticles, spinel, specific magnetization.

For citation: Korsakova A. S., Kotsikau D. A., Haiduk Yu. S., Pankov V. V. Synthesis and physicochemical properties of $Mn_xFe_{3-x}O_4$solid solutions. *Kondensirovannye sredy i mezhfaznye granitsy = Condensed Matter and Interphases*. 2020;22(4): 466–472. DOI: https://doi.org/10.17308/kcmf.2020.22/3076

Для цитирования: Корсакова А. С., Котиков Д. А., Гайдук Ю. С., Паньков В. В. Синтез и физико-химические свойства твердых растворов $Mn_xFe_{3-x}O_4$. *Конденсированные среды и межфазные границы*. 2020;22(4): 466–472. DOI: https://doi.org/10.17308/kcmf.2020.22/3076

✉ Yulyan S. Haiduk, e-mail: j_hajduk@bk.ru (corresponding author)

1. Introduction

The synthesis of nanomaterials has been the focus of many studies lately. Of particular interest are magnetite (Fe_3O_4) and maghemite (γ-Fe_2O_3) magnetic nanoparticles (MNP) [1]. They are used in biotechnology (as drug carriers, biosensors, elements of diagnostic sets, and contrast agents for magnetic resonance imaging), catalysis, electronics, production of magnetic fluids and magnetorheological suspensions, etc. [2, 3]. The magnetic properties of nanoobjects are known to be weaker than those of bulk materials. Thus, their application requires high magnetic characteristics, in particular high saturation magnetisation values. In this regard, magnetite was chosen as one of the best candidates. Moreover, the magnetisation of magnetite may increase due to its ferrous ions being substituted by some transition metals ions. For instance, the magnetic moment of bivalent manganese ions is 5 μB. So, when they replace the magnetite ferrous ions, the magnetic moment of the solid solution may be increased.

At present, there are various methods to obtain oxide nanoparticles [1, 4–9]. The simplest and the most convenient method is the co-precipitation method. It is a well-stidied approach thatallows carrying on the synthesis without heating or using an inert atmosphere. Due to its high sensitivity to various parameters (type of the precipitant, the concentrations of the reagents, pH of the reaction medium, etc.) the method can be used to obtain nanoparticles of various size and properties [1]. It is also quite simple, inexpensive, and practical, and therefore is of great use for large-scale production.

The aim of our study was to obtain single-phased magnetic nanoparticles of $Mn_xFe_{3-x}O_4$ solid solutions at room temperature. We also studied the dependence of the changes in their structure, morphology, and magnetic properties on the degree of substitution in order to determine the compounds with the highest magnetisation values.

2. Experimental

$Mn_xFe_{3-x}O_4$ solid solutions (x = 0; 0.3; 0.6; 0.8; 1.0; 1.2; 1.4; 1.8) were synthesised at room temperature by combined hydrolysis of aqueous solutions of inorganic salts of the corresponding metals. The starting materials ($MnCl_2 \cdot 4H_2O$, $Fe(NO_3)_3 \cdot 9H_2O$, and $FeSO_4 \cdot 7H_2O$) were taken in the stoichiometric proportions (Fe^{3+}: Fe^{2+} = 2: 1 mol.). For some samples, the stoichiometric proportions of the cations Fe^{3+} and Fe^{2+} were altered by 5 % compared to the total number of Fe^{3+} and Fe^{2+}cations. The precipitant was chosen to be NaOH. The amount of the precipitant was 10% larger than the stoichiometric amount. The excess amount of the precipitant was selected specifically so that after mixing the solutions the pH of the reaction mixture was ~ 11. The sample with x = 0.3, which had the highest specific saturation magnetisation, was subjected to thermal treatment in air for 2 h at 300 °C followed by vibromilling (30 min). This was done in order to use the sample to produce a magnetorheological suspension.

The XRD spectra of the powders were registered using a DRON 3.0 diffractometer ($Co_{K\alpha}$-radiation, 1.78897 Å) within angle range of 2θ = 6–80°. The phase composition of the substance was determined by comparing the characteristics of each peak (their diffraction angles and intensity) with the reference values for magnetites Fe_3O_4 (JCPDS 88–0315, a = 8.3752 Å) and $MnFe_2O_4$ (JCPDS 74–2403, a = 8.511 Å). Scherrer's equation was used to calculate the average size of the particles based on the XRD patterns.

The microstructure of the samples was studied using transmission electron microscopes LEO 1420 and HitachiH-800 with an accelerating voltage of 200 keV.

The IR spectra of the samples were registered using an AVATAR 330 (Thermo Nicolet) spectrometer in the region ν = 4000–400 cm^{-1}. The spectra were registered by means of diffuse reflection using a Smart Diffuse Reflectance accessory.

The magnetic characteristics were studied using a Cryogen Free Measurement System from Cryogenic Ltd, where hysteresis loops were recorded at 5 and 300 K, and B_{max} = 8 T.

3. Results and discussion

The spinel structure of a magnetite doped with manganese can be either cubic or tetragonal depending on the degree of substitution. Non-substituted magnetite (x = 0) has a cubic structure, while Mn_3O_4 has a tetragonal lattice [10].

During the transformation from Fe_3O_4 to Mn_3O_4 the degree of inversion of the crystal structure alters, with the magnetite being an inverse spinel and Mn_3O_4 being a normal spinel [7]. This transformation is caused by a different distribution of cations between the sites as suggested in [11]. For $Mn_xFe_{3-x}O_4$, the cation distribution can be generally presented as follows:

$$\left(Mn^{2+}_{x-i}\,Fe^{3+}_{\gamma}\right)_A\left[Mn^{2+}_{i}\,Fe^{2+}_{\gamma-x}\,Fe^{3+}_{2-\gamma}\right]_B O_4, \qquad (1)$$

where x is the degree of substitution in $Mn_xFe_{3-x}O_4$ solid solution (the total number of Mn^{2+}ions); i is the ratio of Mn^{2+} ions in the octahedral sites; and γ is the degree of inversion of the crystal lattice.

It is known that for the stoichiometric manganese ferrite $MnFe_2O_4$ $\gamma = 0.2$, with 80 % of Mn^{2+} ions occupying tetrahedral positions [11].

The XRD patterns of $Mn_xFe_{3x}O_4$ solid solution powders presented in Fig. 1 are similar and have broad peaks. All the synthesised $Mn_xFe_{3-x}O_4$ compounds have a cubic spinel structure, which is characteristic of pure magnetite. The presence of the broad diffraction reflections may result from the low degree of crystallinity of the structure. $Mn_xFe_{3-x}O_4$ with $x > 1.0$ was synthesised using a different method (the stoichiometric proportions of the cations Fe^{3+} and Fe^{2+} were altered by 5 %) to prevent the formation of the α-Fe_2O_3 phase in the samples with high concentrations of manganese ($x > 1.0$).

Despite the low intensity of the peaks, the X-ray diffraction pattern of the sample with x = 1.8 showed a peak at $2\theta = 41.2$, which was assumed to correspond to the diffraction reflection of the spinel with the maximum intensity index (311). The X-ray amorphous state of this compound may indicate a significant deformation of the crystal lattice of the spinel caused by a large number of manganese ions [12]. In other words, it may indicate a gradual structural transformation of the cubic spinel. This study demonstrated that an increase in the degree of substitution is predictably followed by an increase both in unit cell parameters and in its volume. The ionic radius of Mn^{2+} is larger than the one typical of Fe^{2+} and Fe^{3+} regardless of the coordination environment. Therefore, the introduction of manganese ions into the crystal lattice inevitably

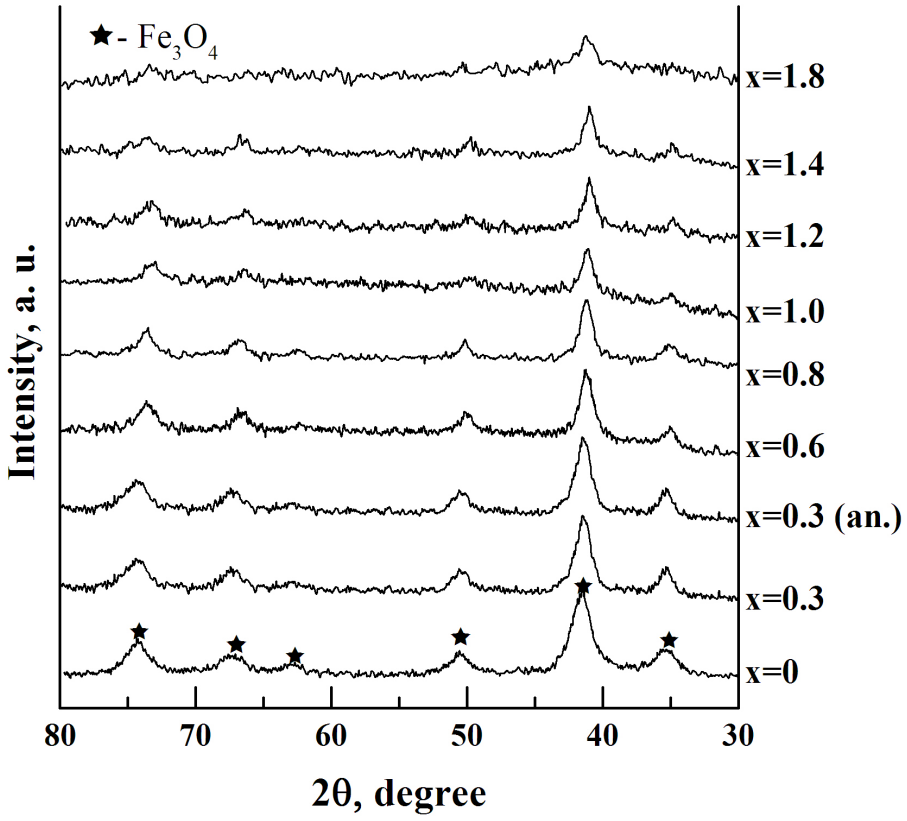

Fig. 1. XRD spectra of $Mn_xFe_{3-x}O_4$ powders ($0 < x < 1.8$)

results in an increase in the unit cell parameters and volume. For the same reason, the peaks with the corresponding Miller indices shift toward the region of narrow angles, when the concentration of manganese in the sample increases.

The calculated lattice constants of the powders with higher concentrations of manganese are smaller than those described in the available literature. The difference can be accounted for by the fact that during the growth of the nanoparticles in alkaline medium and in the presence of atmospheric oxygen, the ageing of the Fe_3O_4 magnetite to γ-Fe_2O_3 maghemite with smaller lattice constant (JCPDS 39–1346, a = 8.3515 Å) proceeds smoothly [13, 14].

The average size of the crystallites increases nonlinearly with an increase in the degree of substitution. The difference in the size may indicate a difference in the speed of $Mn(OH)_2$ and $Fe(OH)_2$ hydrolysis as well as strong competition between them during the formation of nanoparticles of various compositions.

The dislocation densities and the number of micro-stress sites in solid solutions decrease nonlinearly and in a similar way. Micro-stress plays a key role in the development of crystals. They prevent the growth of crystals and thus determine the size if the formed particles [15]. The comparison of the curves showing the alterations in the particle size and micro-stress demonstrates that they are mirror reflections of each other.

Fig. 2 presents TEM microphotographs of some of the samples obtained by the co-precipitation. In each case, nearly spherical nanoparticles were formed. The average size particles of $Mn_{0.3}Fe_{2.7}O_4$ was 9 nm, $Mn_{0.8}Fe_{2.2}O_4$– 11 nm, and $MnFe_2O_4$– 15 nm. The obtained results comply with the average crystallite size calculated using the X-ray diffraction patterns of the corresponding samples. The diameter of the nanoparticles increases with the growth of the concentration of manganese in the $Mn_xFe_{3-x}O_4$ solid solution. For the sample annealed at 300 °C (Fig. 2c), we observed the obvious faceting of the nanoparticles accompanied by an increase in the crystallinity, while the size of the nanoparticles was similar to that of the nanoparticles that had not been annealed.

For the spinel structures, the characteristic IR spectra lines indicating the presence of structural changes correspond to the vibrations of M–O and M–O–H bonds. The ion environment of Fe^{3+} was altered by introducing divalent ions with large radii into the magnetite crystal lattice. This resulted in the distortion of the symmetry of the coordination environment of Fe^{3+} or changes in the force constant of the Fe–O bond. Therefore, the IR spectra (Fig. 3) demonstrate the splitting or distortion of the lines of characteristic vibrations of the Fe–O bond. When manganese and iron ions are evenly distributed within the crystal lattice of the spinel, one can usually observe the shift of the absorption peaks of characteristic vibrations only. The additional peaks indicate the presence of a different phase.

The results of the IR spectroscopy presented in Fig. 3 confirm the formation of the spinel structure for all the compounds.

The characteristic frequencies ν_1 (≈ 560 cm^{-1}) and ν_2 (≈ 430 cm^{-1}) corresponding to the stretching vibrations of Me–O in tetrahedral and octahedral

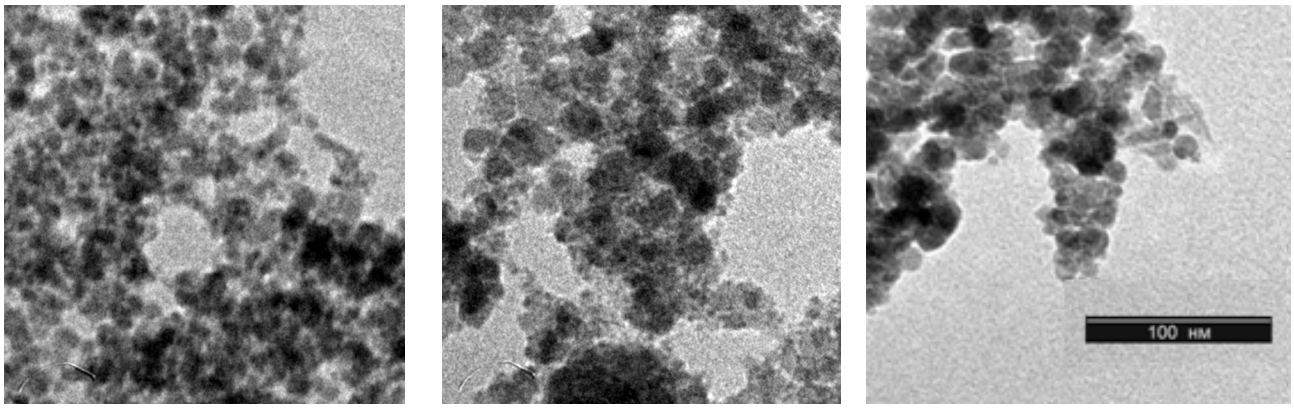

a *b* *c*

Fig. 2. TEM images of the $Mn_xFe_{3-x}O_4$ powder: a) x = 0.3; b) x = 1.0; c) x = 0.3 (annealed at 300 °C, 2 h)

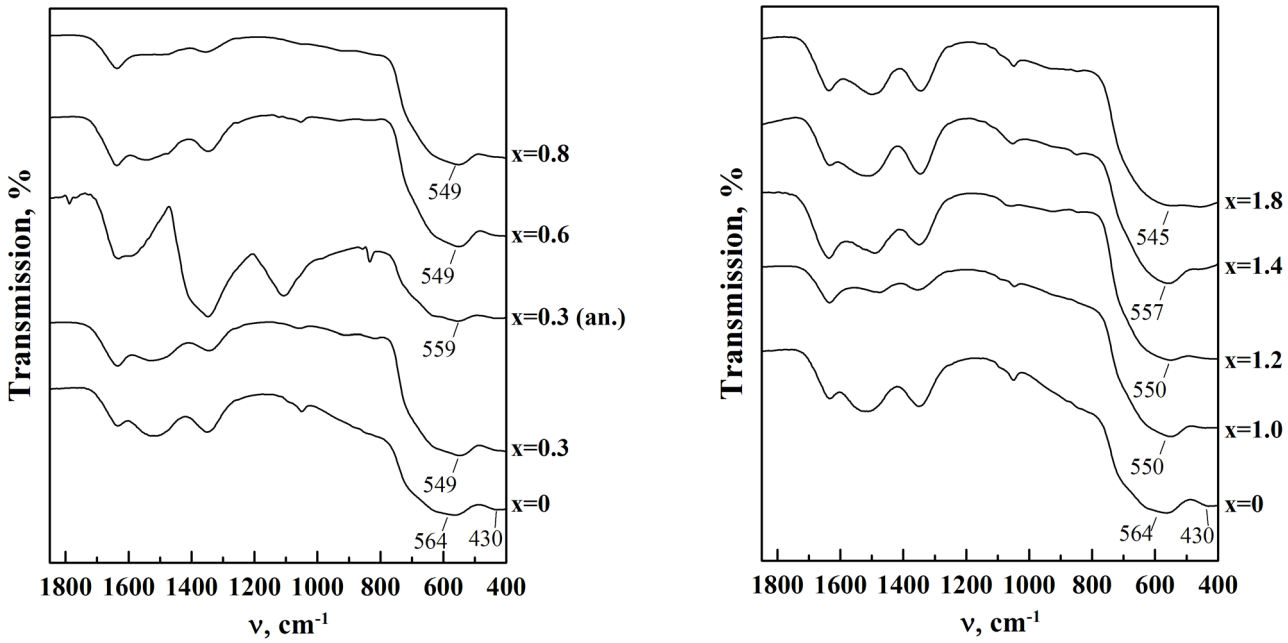

Fig. 3. Fragments of IR spectra of $Mn_xFe_{3-x}O_4$ solid solutions ($0 < x < 1.8$), (an.) – the powder after annealing at 300 °C for 2 h

sites shift towards lower frequencies after the introduction of Mn^{2+}cations. This is caused by the presence of combined vibrational bands of the Fe–O bonds in octahedral positions with Mn^{2+} ions in the immediate coordination environment Fe–O–Mn. This results in the increase in the length of the bond ($l_{Mn\text{-}O} > l_{Fe\text{-}O}$) and alters the force constant.

For samples with a high manganese content ($x > 1.2$), as well as for a sample with $x = 0.3$ (an.), a low-intensity band at 848.57 cm^{-1} was found, characteristic of the individual oxide α-Fe_2O_3. X-ray diffraction analysis did not reveal this phase in the samples.

The magnetic properties of the $Mn_xFe_{3-x}O_4$ nanoparticles were analysed using the experimental data on their specific magnetisation and coercivity in the temperature range of 5–300 K. The magnetisation and demagnetisation curves were similar at room temperature, which proves the absence of hysteresis and coercive force, and indicates a superparamagnetic state of the nanoparti-

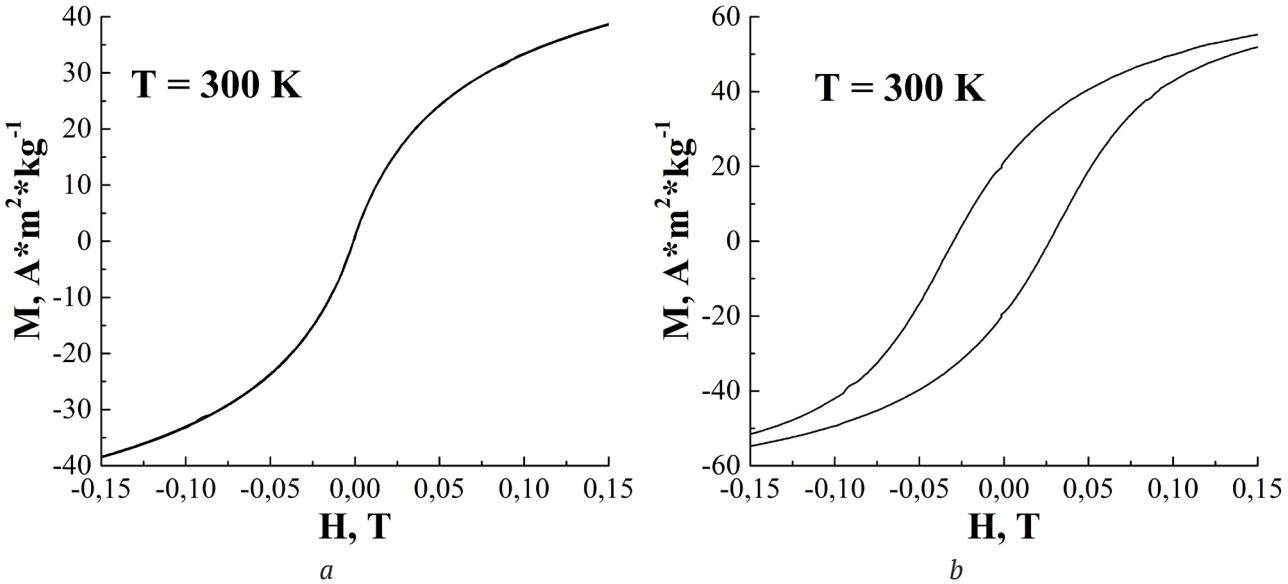

Fig. 4. Curves of specific saturation magnetisation for the $Mn_{0.3}Fe_{2.7}O_4$ sample at 300 K and the $Mn_{0.3}Fe_{2.7}O_4$ sample (annealed at 300 °C, 2 h) at 300 K

cles (Fig. 4a). At the same time, $Mn_{0.3}Fe_{2.7}O_4$ sample annealed at 300 °C for 2 hours had a coercivitye of ~ 120 Oe (Fig. 4b). Therefore, thermal treatment results in further crystallisation and an increase in the anisotropy constant.

The magnetic properties of the $Mn_xFe_{3-x}O_4$ solid solutions depend directly on the distribution of cations within the spinel structure [7]. The distribution is of combined nature, i.e. manganese ions occupy both tetrahedral and octahedral sites of the crystal lattice. Thus, for the manganese ferrite the distribution is $(Mn_{0.8}Fe_{0.2})$ $[Mn_{0.2}Fe_{1.8}]O_4$.

The saturation magnetisation changes nonlinearly with an increase in the concentration of manganese in $Mn_xFe_{3-x}O_4$. The magnetisation grows at first following the increase in the portion of manganese in the solid solution. It reaches its maximum for $Mn_{0.3}Fe_{2.7}O_4$ compound and then decreases (Fig. 5).

The dependence occurs because the magnetic moment of the Mn^{2+} ion (5 μB) with five unpaired electrons is higher than that of the Fe^{2+} ion (4 μB). Therefore, when Fe^{2+} ions are replaced with Mn^{2+} ions in the octahedral sub-lattice, the magnetisation should grow. The saturation magnetisation is mainly determined by the superexchange interaction between the ions of A and B sub-lattices, which can be described using the formula

$$\mu_{theor} = \mu_B - \mu_A, \quad (2)$$

where μ_A and μ_B are the magnetic moments of the cations of A and B voids respectively.

If the number of manganese ions in $Mn_xFe_{3-x}O_4$ increases further, the ions being oxidised to Mn^{3+} actively begin to occupy the B voids of the crystal lattice. Since Fe^{3+} = (5 μB) and Mn^{3+} = (4 μB), the super-exchange interaction between the ions in sub-lattices A and B decreases, which in turn leads to a decrease in the saturation magnetisation of $Mn_xFe_{3-x}O_4$.

4. Conclusions

The study allowed us to determine the conditions for the synthesis of single-phase magnetite nanoparticles doped with manganese at room temperature and under atmospheric pressure. The concentrations at which solid solutions of iron and manganese oxides have the structure of a cubic spinel lie within the range

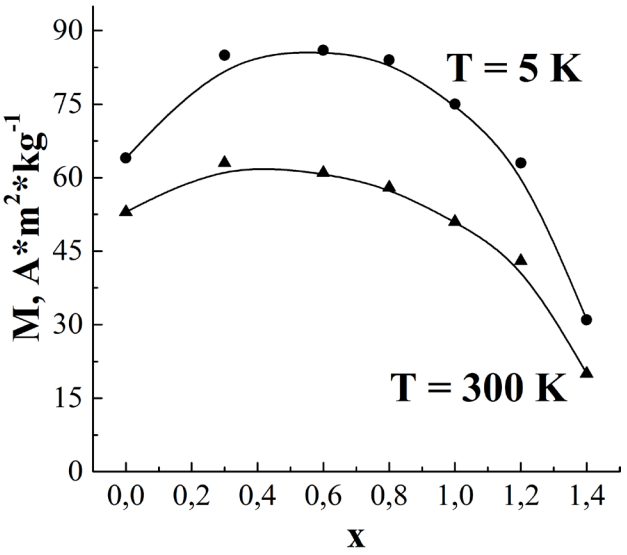

Fig. 5. Specific magnetisation of $Mn_xFe_{3-x}O_4$ solid solutions depending on the compound

$0 < x < 1.8$.

The alteration in the saturation magnetisation caused by an increase in the concentration of manganese oxide in the solid solution is nonlinear. The maximum saturation magnetisation (68 А·м²·kg⁻¹ at 300 K and 85 А·м²·kg⁻¹ at 5 K) was observed in $Mn_{0.3}Fe_{2.7}O_4$. The smallest nanoparticles (9 nm) are observed in $Mn_{0.3}Fe_{2.7}O_4$.

The synthesised nanoparticles can be used as contrast agents for MRI diagnostics and as components of magnetorheological fluids, as well as to obtain magnetorheological fluids and produce magnetically controlled capsules for targeted drug delivery.

Conflict of interest

The authors declare that they have no known competing financial interests or personal relationships that could have influenced the work reported in this paper.

References

1. Gubin C. G., Koksharov Yu. A., Khomutov G. B., Yurkov G. Yu. Magnetic nanoparticles: preparation, structure and properties. *Russian Chemical Reviews* 2005;74(6): 539–574. Available at: https://www.elibrary.ru/item.asp?id=9085819

2. Skumryev V., Stoyanov S., Zhang Y., Hadjipanayis G., Givord D., Nogués J. Beating the superparamagnetic limit with exchange bias. *Nature.* 2003;423(6943): 850–853. DOI: https://doi.org/10.1038/nature01687

3. Joseph A., Mathew S. Ferrofluids: synthetic strategies, stabilization, physicochemical features,

characterization, and applications. *ChemPlusChem*. 2014;79(10): 1382–1420. DOI: https://doi.org/10.1002/cplu.201402202

4. Mathew D. S., Juang R.-S. An overview of the structure and magnetism of spinel ferrite nanoparticles and their synthesis in microemulsions. *Chemical Engineering Journal*. 2007:129(1–3): 51–65. DOI: https://doi.org/10.1016/j.cej.2006.11.001

5. Rewatkar K. G. Magnetic nanoparticles: synthesis and properties. *Solid State Phenomena*. 2016:241: 177–201. DOI: https://doi.org/10.4028/www.scientific.net/ssp.241.177

6. Tartaj P., Morales M. P., Veintemillas-Verdaguer S., Gonzalez-Carre´no T., Serna C. J. The preparation of magnetic nanoparticles for applications in biomedicine. *Journal of Physics D: Applied Physics*. 2003:36(13): 182–197. DOI: https://doi.org/10.1088/0022-3727/36/13/202

7. West A. *Khimiya tverdogo tela. Teoriya i prilozheniya [Solid State Chemistry and Its Applications]*. In 2 parts Part 1. Transl. from English. Moscow, Mir, 1988 558 p.

8. *Spravochnik khimika: V 6 t. 2-e izd. Obshchiye svedeniya. Stroyeniye veshchestva. Svoystva vazhneyshikh veshchestv. Laboratornaya tekhnika* [Chemist's Handbook: In 6 volumes, 2nd ed. General information. The structure of matter. Properties of the most important substances. Laboratory equipment]. B. P. Nikolskiy (ed.) Moscow – Leningrad: Goskhimizdat Publ.; 1963. V. 1. 1071 p. (In Russ.)

9. Zhuravlev G. I. *Khimiya i tekhnologiya ferritov* [Ferrite chemistry and technology]. Leningrad: Khimiya Publ.; 1970. p. 192. (In Russ.)

10. Mason B. Mineralogical aspects of the system FeO-Fe_2O_3-MnO-Mn_2O_3. *Geologiska Föreningen i Stockholm Förhandlingar*. 1943;65(2): 97–180. DOI: https://doi.org/10.1080/11035894309447142

11. Guillemet-Fritsch S., Navrotsky A., Tailhades Ph., Coradin H., Wang M. Thermochemistry of iron manganese oxide spinels. *Journal of Solid State Chemistry*. 2005;178(1):106–113. DOI: https://doi.org/10.1016/j.jssc.2004.10.031

12. Ortega D. Structure and magnetism in magnetic nanoparticles. In: *Magnetic Nanoparticles: From Fabrication to Clinical Applications*. Boca Raton: CRC Press; 2012. p. 3–72. DOI: https://doi.org/10.1201/b11760-3

13. Kodama T., Ookubo M., Miura S., Kitayama Y. Synthesis and characterization of ultrafine Mn(II)-bearing ferrite of type $Mn_xFe_{3-x}O_4$ by coprecipitation. *Materials Research Bulletin*... 1996:31(12): 1501–1512. DOI: https://doi.org/10.1016/s0025-5408(96)00146-8

14. Al-Rashdi K. S., Widatallah H., Al Ma'Mari F., Cespedes O., Elzain M., Al-Rawas A., Gismelseed A., Yousif A. Structural and mossbauer studies of nanocrystalline Mn^{2+} doped Fe_3O_4 particles. *Hyperfine Interact*. 2018:239(1): 1–11. DOI: https://doi.org/10.1007/s10751-017-1476-9

15. Modaresi N., Afzalzadeh R., Aslibeiki B., Kameli P. Competition between the Impact of cation distribution and crystallite size on properties of $Mn_xFe_{3-x}O_4$ nanoparticles synthesized at room temperature. *Ceramics International*. 2017:43(17): 15381–15391. DOI: https://doi.org/10.1016/j.ceramint.2017.08.079

Information about the authors

Alina S. Korsakova, intern, research fellow, Research Institute for Physical Chemical Problems of the Belarusian State University, Minsk, Republic of Belarus; e-mail: korsakova@bsu.by. ORCID iD: https://orcid.org/0000-0001-8898-4726.

Dzmitry A. Kotsikau, PhD in Chemistry, Associate Professor, Belarusian State University, Minsk, Republic of Belarus; e-mail: kotsikau@bsu.by. ORCID iD: https://orcid.org/0000-0002-3318-7620.

Yulyan S. Haiduk, research fellow, Belarusian State University, Minsk, Republic of Belarus; e-mail: j_hajduk@bk.ru. ORCID iD: https://orcid.org/0000-0003-2737-0434.

Vladimir V. Pankov, DSc in Chemistry, Professor, Head of the Department of Physical Chemistry, Belarusian State University, Minsk, Republic of Belarus; e-mail: pankov@bsu.by. ORCID iD: https://orcid.org/0000-0001-5478-0194.

All authors have read and approved the final manuscript.

Translated by Yulia Dymant
Edited and proofread by Simon Cox